

## Chapter 4

### The Colorado Student Space Weather Experiment

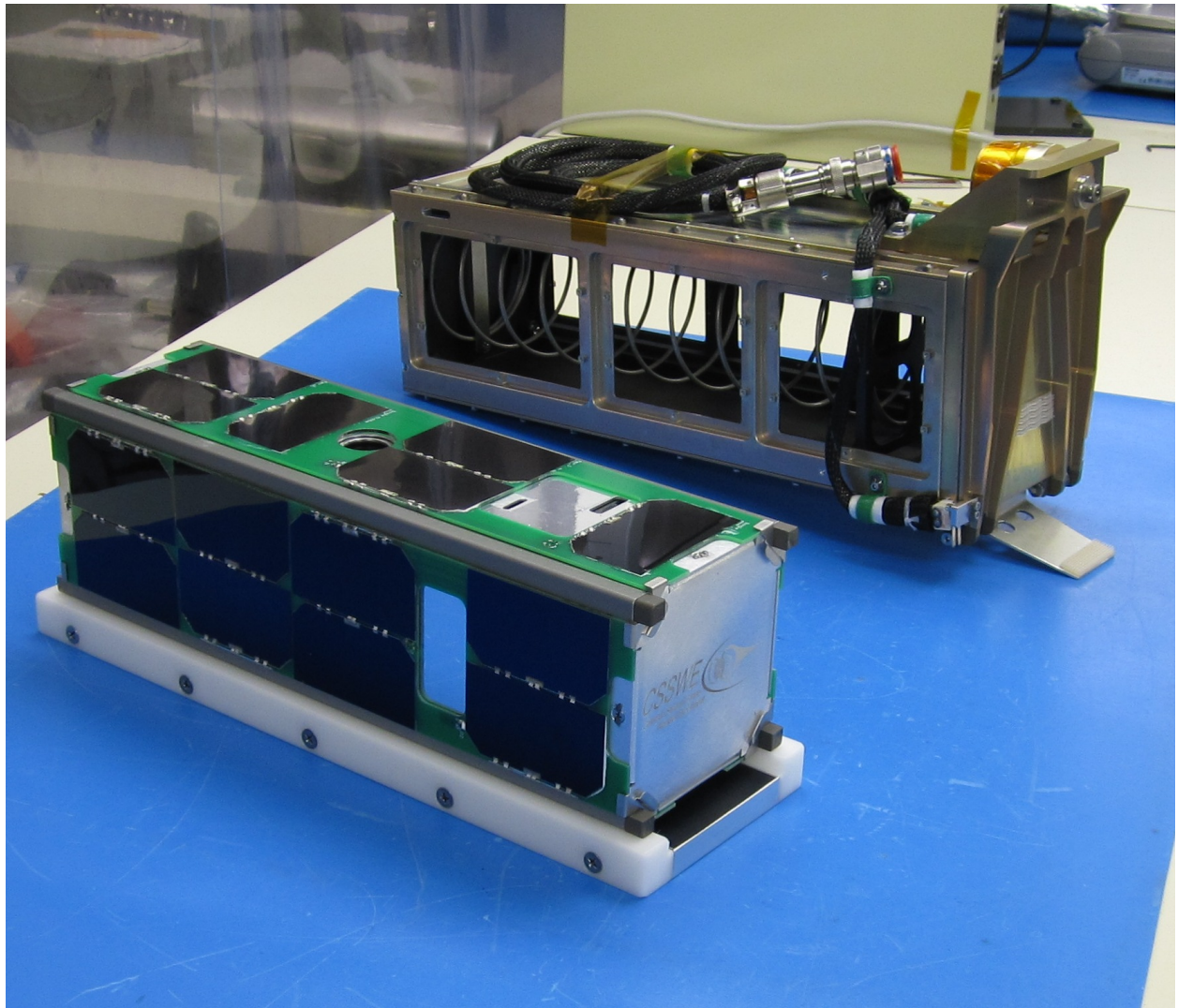
The Colorado Student Space Weather Experiment (CSSWE) is a 3U CubeSat [75] built at the University of Colorado Boulder as a joint project between the department of Aerospace Engineering Sciences (AES) and the Laboratory for Atmospheric and Space Physics (LASP). Involvement with CSSWE served as the motivation for this dissertation topic. CSSWE uses Passive Magnetic Attitude Control (PMAC) and we have full access to the satellite data. Thus, this CubeSat is an important feature of this dissertation.

CSSWE was selected for funding from the National Science Foundation in spring of 2010. Following a two year period of design, build, and test, CSSWE was delivered for PPOD integration in January 2012. Figure 4.1 shows an image of CSSWE and the Poly-Picosat Orbital Deployer (P-POD) launch device as captured during delivery. On September 13, 2012, CSSWE was inserted into a  $478\text{km} \times 786\text{km}$ ,  $64.7^\circ$  inclination orbit as part of the NASA Educational Launch of Nanosatellites (ELaNa) VI launch [68]. CSSWE launched as a secondary payload aboard an Atlas V rocket operated by the United Launch Alliance (ULA) with a primary payload from the National Reconnaissance Office (NRO).

#### 4.1 Science Mission Success

The science objectives of CSSWE are to investigate the relationship of the location, magnitude, and frequency of solar flares to the timing, duration, and energy spectrum of solar energetic particles reaching Earth and to determine the precipitation loss and the evolution of the energy spec-

Figure 4.1: The Colorado Student Space Weather Experiment (CSSWE, bottom left) CubeSat and its launch device, the Poly-Picosat Orbital Deployer (P-POD, upper right)



trum of radiation belt electrons [50]. To accomplish these objectives, CSSWE carries a miniaturized version of the Relativistic Electron and Proton Telescope (REPT), developed by LASP engineers for Van Allen Probes mission. CSSWE's lone science instrument, the Relativistic Electron and Proton Telescope *integrated little experiment* (REPTile, shown in Figure 4.2), uses 350V-biased silicon detectors to measure the directional differential flux of electrons from 0.5 to  $>3$  MeV and protons from 10 to 40 MeV within a  $52^\circ$  field of view [66]. The data product of the mission is count rates for each particle within four energy bins, generated every six seconds.

The REPTile instrument measures charged particles which revolve around magnetic field lines as they travel. Thus, passive magnetic attitude control is beneficial because it results in higher particle count rates because the instrument field of view is oriented perpendicular to the local magnetic field direction. Also, the non-isotropic CSSWE antenna pattern favors alignment with the local magnetic field, which ensures an RF link can be established the majority of the time CSSWE is visible to the ground station in Boulder, CO.

The CSSWE mission has proven highly successful [49]. CSSWE proposed a mission lifetime of four months: one month of spacecraft checkout with full mission success defined by three months of science operations. As of Christmas Eve 2013, the satellite remains operational 466 days after launch with the science mission extended to over three times the 90 day full mission success duration. CSSWE is the quintessential proof that high-impact, journal-quality science can be accomplished with a low-cost CubeSat [48].

## 4.2 Coordinate System

CSSWE uses the body-fixed coordinate system shown in Figure 4.3. With the origin at the center of mass, the CSSWE X-, Y-, and Z-axes are aligned with the satellite major, intermediate, and minor inertia axes, respectively. The CSSWE principle inertia matrix about the center of mass is shown below; note that the satellite is close to symmetric about the X- and Y-axes.

Figure 4.2: The REPTile instrument collects particles in its  $52^\circ$  field of view through the collimator (C). Off-axis electrons are reflected by the collimator teeth away from the aperture. A beryllium window (F) absorbs electrons  $< 500$  keV and protons  $< 10$  MeV, preventing detector saturation. Particles travel through the detector stack (E), depositing energy on each detector as they travel. Binning logic allows the calculation of particle energy based on detector stack penetration. Aluminum (A) and Tungsten (B) shielding enclosing the detector stack limits noise due to particles not in the REPTile field of view. Three Tantalum alignment pins (D) provide rotational stability for the detector stack while providing the necessary shielding.

- A. Aluminum Outer Shielding
- B. Tungsten Inner Shielding
- C. Tantalum Collimator and Baffles
- D. Tantalum Alignment Pin
- E. Silicon Detectors
- F. Beryllium Window

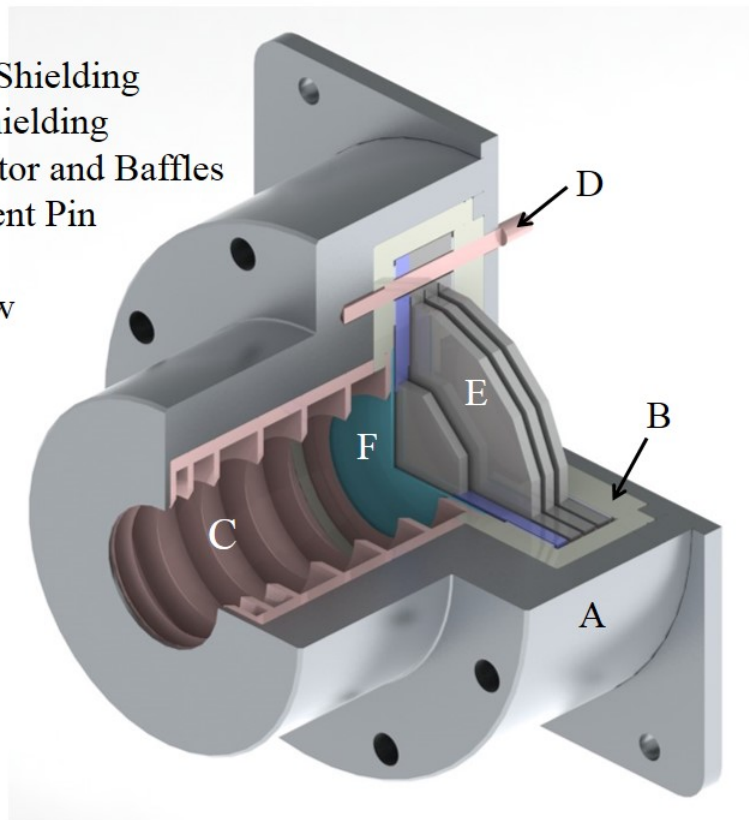
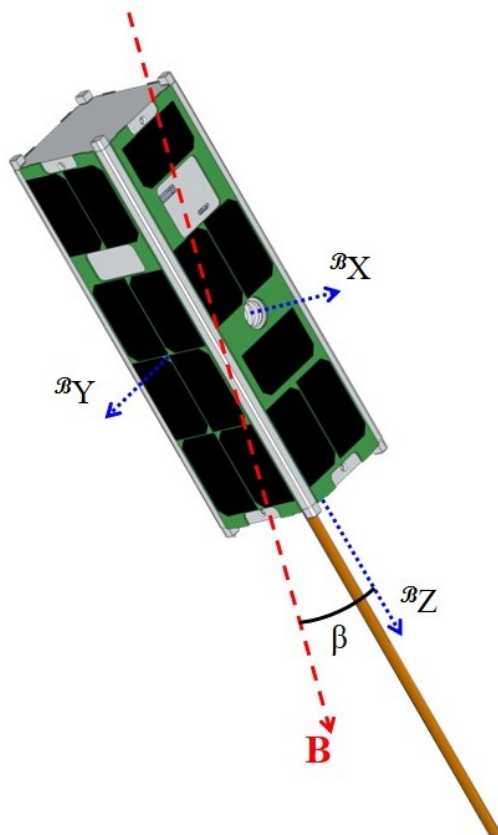


Figure 4.3: The CSSWE coordinate frame is shown with the definitions for  $\alpha$  and  $\beta$  error angles. The body X-axis  ${}^B X$  is aligned with the REPTile aperture, the body Z-axis  ${}^B Z$  is aligned with the deployed antenna, and the body Y-axis  ${}^B Y$  is defined by the right-hand rule. The angle  $\beta$  exists between the body frame  $+{}^B Z$  axis and magnetic flux density vector  $\mathbf{B}$ . The  $\beta$  angle is referenced throughout this document.



$$[I] = \begin{bmatrix} 0.0222 & 0 & 0 \\ 0 & 0.0218 & 0 \\ 0 & 0 & 0.0050 \end{bmatrix} \text{ kg} \cdot \text{m}^2.$$

### 4.3 Sensors and Telemetry

The satellite sensors are split into two types: housekeeping and attitude. The housekeeping sensors measuring temperature, current, and voltage throughout the spacecraft. The attitude sensors are used to measure the 3-axis local magnetic field vector and the partial sun position vector.

#### 4.3.1 Housekeeping

CSSWE contains 38 housekeeping sensors spread throughout the satellite; Table 4.1 shows each sensor and its associated Analog to Digital Converter (ADC). Each ADC digitizes the analog readings with an 8-bit resolution. CSSWE queried each of these sensors once per minute and used these readings to compile ten-minute mean, maximum, and minimum values for each sensor. The sensors are detailed because some are used for magnetometer calibration (Section 4.3.2) while others are helpful for validating the attitude filter output (Section 6.3.2).

#### 4.3.2 Attitude

The raw attitude measurements are not used by the satellite on-orbit; instead, they are transmitted to the ground for post-processing. Chapter 6 describes the ground-based satellite attitude determination using sensor output. This section focuses solely on the CSSWE attitude sensor hardware, output, and calibration.

CSSWE uses a three-axis magnetometer (Honeywell HMC5883L) and four photodiodes (Vishay TEMD6010FX01) to determine the full local magnetic flux density vector and the partial sun vector, respectively. The magnetometer is digitized with a 12-bit ADC, while the photodiodes share

Table 4.1: The 38 CSSWE housekeeping sensors are detailed below. Each sensor output is quantized by an 8-bit analog to digital converter before recording to memory. Attitude sensors are not included in this table, but ADC1 also digitizes the four photodiodes.

Analog to Digital Converter	Sensor	Quantity
ADC1	Solar Panel Temperature	4
ADC2	Solar Panel Voltage	4
	Solar Panel Current	4
ADC3	Battery Voltage	1
	Battery Temperature	1
	Battery Charge Current	1
	Battery Discharge Current	1
	5V Buck Voltage	1
	5V Buck Current	1
	3.3V Buck Voltage	1
	3.3V Buck Current	1
ADC4	REPTile Detector Voltage	4
	REPTile Detector Current	4
ADC5	REPTile Detector 1 Temperature	1
	REPTile Board Temperature	1
	REPTile Reference Voltage	3
	3.3V Buck Voltage at REPTile	1
Radio	Microcontroller Temperature	1
	Power Amp Temperature	1
	RSSI	1
C&DH	Microcontroller Temperature	1

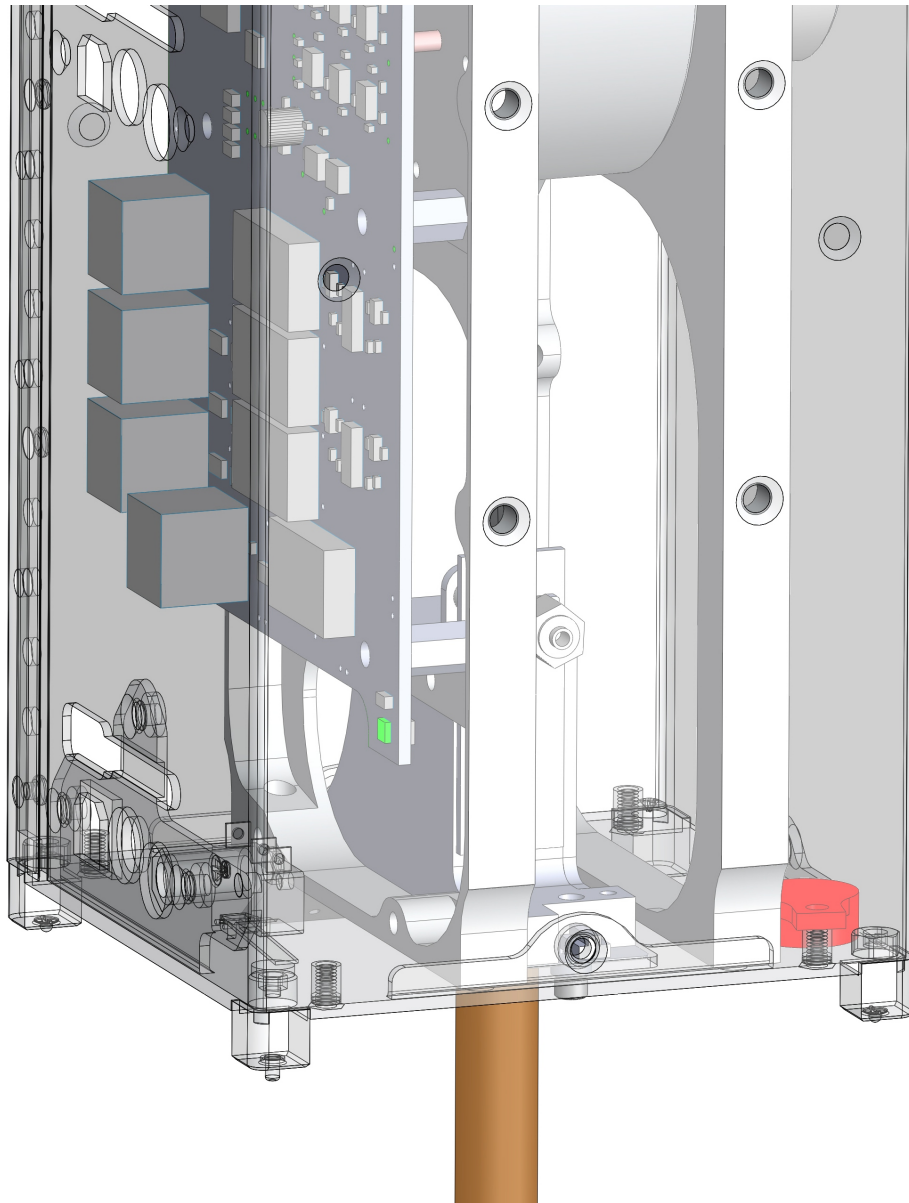
the 8-bit ADC1 used by the solar panel temperature sensors (see Table 4.1). The instantaneous attitude sensors output values are recorded once every six seconds.

#### 4.3.2.1 Magnetometer

The magnetometer was calibrated before flight using a time-invariant, attitude-independent method [31] which accounts for the offset, scale factor, and non-orthogonality biases. To account for temperature, current, and science instrument biases, a time-varying, attitude-independent calibration method was applied [72]. This calibration uses the first three days on-orbit (while the satellite is still covering the majority of the attitude sphere) to fit static calibration parameters based on time-varying telemetry. The Command and Data Handling (C&DH) board temperature telemetry is used as a proxy for the magnetometer temperature. Although a ten-minute average is the highest temporal resolution available for housekeeping data, it is found to be sufficient to correct for scale and offset magnetometer temperature errors. Post-launch analysis shows that the magnetometer temperature is the most significant source of time-varying error. The 10 minute average battery voltage telemetry is used as a proxy for system currents near the magnetometer which generate offset errors. The final magnetometer offset correction is based on the activation status of the REPTile instrument. The magnetometer is sensitive to REPTile currents because it is located on the REPTile electronics board, as shown in Figure 4.4. Also shown is the magnetometer proximity to the steel-tape communications antenna which deploys two hours after PPOD ejection. The antenna deployment changes the magnetic moment of the spacecraft (see Section 6.3.2.1) and has a significant effect on the magnetometer calibration.

Figure 4.5 shows the magnetometer B-field magnitude error over the first thirty days of on-orbit operations with various calibrations applied. The error is calculated as the difference between the measured B-field magnitude and the International Geomagnetic Reference Field (IGRF) magnetic model output magnitude (see Section 8.1.5.1). Relative to the daily average magnitude of the IGRF, the raw data has a daily average error of well over 400% and is thus unusable. The ground-based calibration reduces the daily average error to about 15%, or about  $9^\circ$  of attitude er-

Figure 4.4: Solid model of the magnetometer (green) position relative to the bar magnet (red) and the deployed antenna (copper). The magnetometer is sensitive to REPTile currents due to its placement on the REPTile electronics board.



ror. The on-orbit, time-varying calibration is the only dataset with a mean error below its standard deviation. The maximum net effect of the measurement error average and standard deviation is about a 2% error relative to the daily average IGRF magnitude, or about a  $1.1^\circ$  attitude error.

#### 4.3.2.2 Photodiodes

CSSWE has photodiodes on each of its 3U faces ( $+^B X$ ,  $-^B X$ ,  $+^B Y$ ,  $-^B Y$ ); these allow for a partial sun vector measurement. Each photodiodes measures the sun direction by assuming 1) an output when the sun is perpendicular and 2) that the output decreases as a cosine with the sun direction. However, the second assumption is usually invalid at high incidence angles due to physical limitations (refraction, manufacturing imperfections, etc.) and secondary light sources. As a result, CSSWE does not use photodiode measurements beyond a  $70^\circ$  field of view. Figure 4.6 shows the relationship between the number of illuminated photodiodes and the sun direction vector in the body frame; this figure has slight inaccuracies due to the size of each grid element (which are large for clarity purposes).

The photodiodes were calibrated using an attitude-dependent, batch-based approach using on-orbit data which takes into account the effects of albedo. This calibration is largely based on the work of Springmann [70]. However, partial sun vector measurement based on the four CSSWE photodiodes is not sufficient to estimate the photodiode calibration parameters when directly included as filter states. Instead, a novel batch-based filtering approach is used to calibrate each photodiode (for more information, see Section 6.2.2). This calibration corrects for the scale factor and misalignment angles of each photodiode. The misalignment angles account for manufacturing and mounting defects; these parameters do not change with time.

The scale factor is defined as the output from a photodiode when it is perpendicular to the sun alone (no albedo); this parameter changes over time. Figure 4.7 shows that the photodiodes experience significant degradation over the first month on orbit; this degradation is believed to be due to UV light darkening the plastic covering of each photodiode. The figure also shows that the scale factor of each photodiode is recalculated every six hours to account for degradation as

Figure 4.5: The difference in magnetic flux density magnitude as measured by the CSSWE magnetometer vs. predicted by the International Geomagnetic Reference Field (IGRF, see Section 8.1.5.1) model. Both the daily mean error (filled squares) and the daily standard deviation of the error (open circles) are shown. The black lines are the maximum and minimum modeled B-field magnitude at the CSSWE orbit each day. Red is the error of the raw data from the magnetometer, blue is the error after the ground-based (static calibration parameters) calibration is applied, and green is the error after the on-orbit (dynamic calibration parameters) calibration is applied.

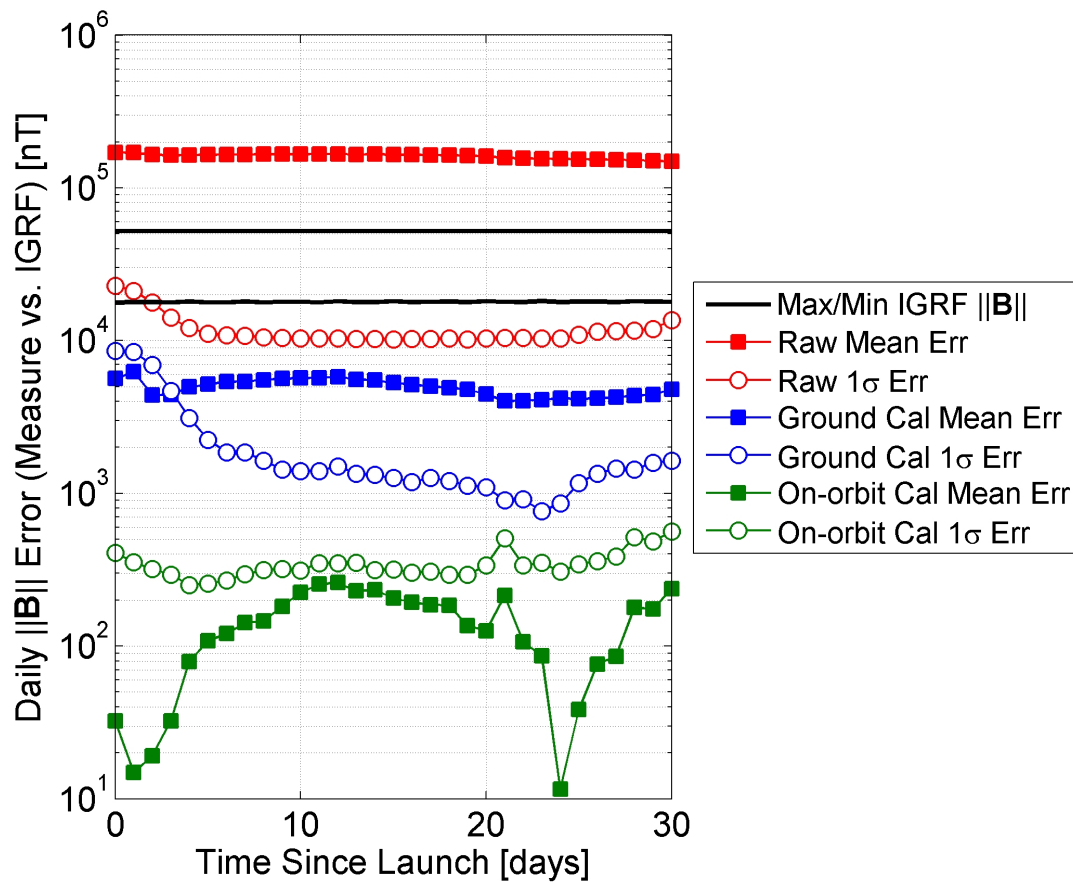
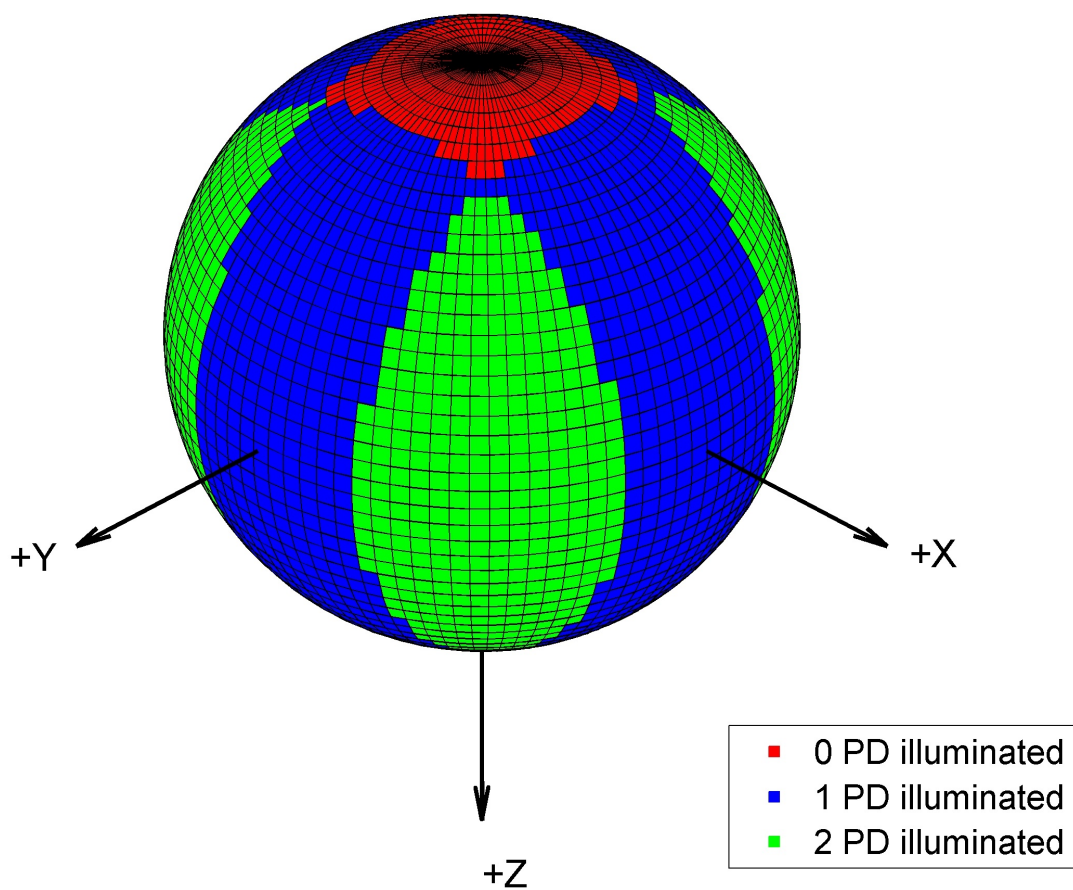


Figure 4.6: The number of illuminated photodiodes given a sun direction vector for the CSSWE CubeSat. This distribution assumes photodiodes with a  $70^\circ$  field of view aligned with the  $+X$ ,  $-X$ ,  $+Y$ , and  $-Y$  axes.



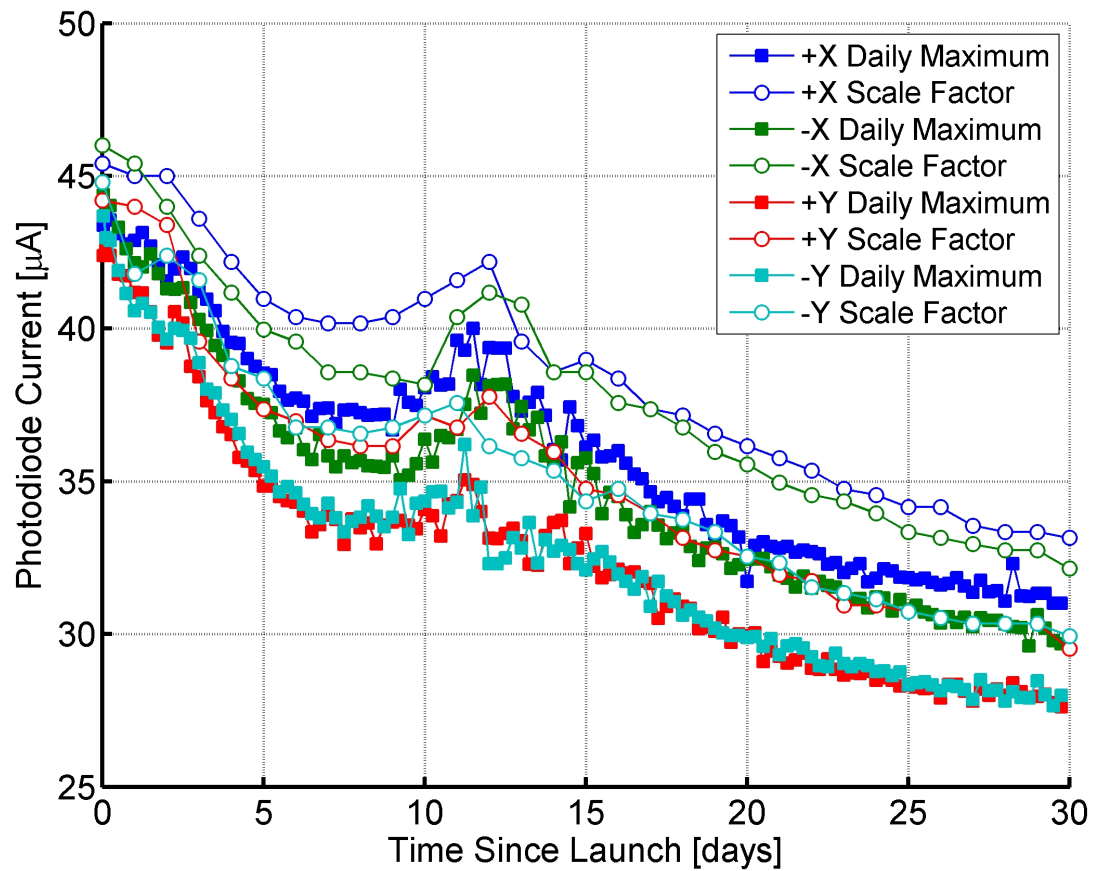
it occurs. After calibration, the photodiodes have a nominal 1-sigma standard deviation of  $1.6\mu\text{A}$  due primarily to the uncertainty of the albedo model. In the early mission, the maximum sun-only current is about  $45\mu\text{A}$  (equivalent to about  $2.0^\circ$  of attitude error) but by late mission this maximum sun-only current decreases to about  $32\mu\text{A}$  (equivalent to about  $2.8^\circ$  of attitude error).

#### 4.3.2.3 Inertial Models and Uncertainties

The measurements cannot be used to determine spacecraft attitude without some estimate of their inertial values. CSSWE uses a Two Line Element (TLE) set with the SPG4 propagator for position information (see Section 8.1.4). The satellite position is used to generate both the inertial sun vector (accurate to  $0.01^\circ$ ) and the inertial magnetic field vector (accurate to about  $1^\circ$  as shown below); both models are explained in more detail in Section 8.1.5.

Figure 4.8 shows the results of an investigation of the Two Line Element (TLE) set uncertainty over the first 30 days on orbit. The TLE is propagated to determine the satellite position and velocity at a given time (see Section 8.1.4); thus an inaccurate TLE will lead to an inaccurate position estimate. This investigation was performed by simulating CSSWE dawn crossings and comparing each crossing with on-orbit photodiode data. Red lines have been added to the figure at  $\pm 6$  seconds to show the expected variation in dawn crossings as CSSWE records photodiode data once every six seconds. The figure shows that the CSSWE TLE-based position degrades over the first month on orbit. During this time period, CSSWE drifts apart from the other 10 CubeSats from the same launch; this may have caused issues for the tracking agency which supplies the TLEs. Regardless, the data shows that the simulated dawn crossings have errors as high as 18s compared to the measurements. Simulations of the first month's orbit show that an 18s in-track position error results in IGRF model errors with a  $1\sigma$  standard deviation of 284nT. However, this is a worst case that is seldom experienced; a more reasonable assumption is a 10s in-track position error, resulting in IGRF model errors of 158nT. The IGRF model can also differ from truth in the presence of geomagnetic storms. Moderate storms can cause variations up to 100nT at low latitudes [51]. Recent analysis has shown high latitudes can experience variations of up to 1000nT

Figure 4.7: The maximum recorded output current for each photodiode is shown with the open circles. The filled squares show the scale factor for each photodiode, which was fit to the on-orbit data every six hours. The photodiode scale factor is the current that would be registered by the photodiode if it were perpendicular to the sun alone (no albedo).



during moderate storms [42]. Because the attitude determination is performed via post-processing, the storm-based magnetic field variation can be avoided by selectively processing datasets during which geomagnetic activity is low. For comparison, the lowest magnetic flux density magnitude experienced within the CSSWE orbit is about  $18\mu\text{T}$ , so  $180\text{nT}$  is equivalent to 1% error or about  $0.57^\circ$  angular error.

#### 4.4 Latch-up Anomaly

Although CSSWE met all of its goals for full mission success, it did have setbacks. The most severe anomaly (with implications for attitude determination) began on October 14, 2012, at 23:28:45 UTC. Based on received telemetry, it is believed that ADC4 (see Table 4.1) experienced a latch-up anomaly, likely due to a high-energy particle impact. The latch-up caused an undesired low impedance path to ground through ADC4. This short circuit eventually brought the battery voltage below a battery protection circuitry threshold, triggering a system reset which cleared the latch-up two hours after the anomaly began. As a result of the anomaly, ADC4 was destroyed and both ADC1 and ADC2 were damaged. Unfortunately, ADC1 digitizes the photodiode output, which was degraded by the anomaly. Figure 4.9 shows the raw bit-level output from ADC1 before and after the latch-up anomaly occurs in mid October. The +X, -X, and +Y photodiodes lose certain bits after the anomaly. As a result, there is increased quantization of the photodiode output, greatly reducing its usefulness in attitude estimation. For an 8-bit ADC (maximum output 255), losing bit 5 (+X, -X) or 7 (+Y) results in percent errors of 12.5% or 50.1%, respectively. Because the attitude determination relies upon accurate photodiode output, the CSSWE three-axis attitude is limited to the first month of on-orbit operations.

Figure 4.8: The difference between the dawn crossing predicted by the current Two Line Element (TLE) set and the photodiode-based dawn crossing observation. The green dots are the closest dawn crossing to an updated TLE; the blue dots are propagated forward or backward in time using data from the most recent TLE. Dotted red lines are visible at  $\pm 6$  sec to indicate the photodiode measurement period; differences beyond these boundaries are likely due to errors in TLE-based position. The increasing error is thought to be due to the ten CubeSats launched with CSSWE dispersing over time.

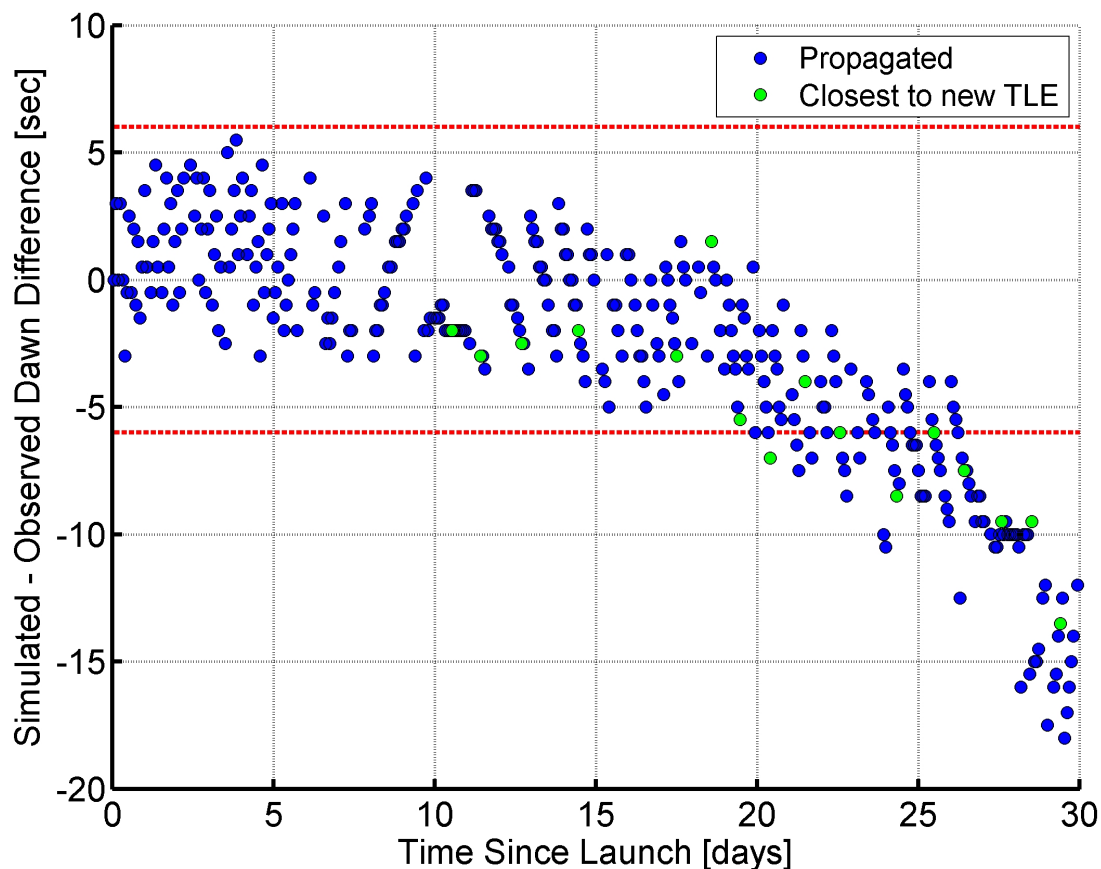


Figure 4.9: The output of ADC1 before and after the latch-up anomaly. Select bits are no longer active after the anomaly, causing increased quantization of the output data. The +X and -X photodiodes lose bit 5 while the +Y photodiode bit 7 becomes intermittent.

